Catalytic mechanism of the glutathione peroxidase-type tryparedoxin peroxidase of *Trypanosoma brucei*

Tanja SCHLECKER*, Marcelo A. COMINI*, Johannes MELCHERS*, Thomas RUPPERT† and R. Luise KRAUTH-SIEGEL*[1]

*Biochemie-Zentrum der Universität Heidelberg, Im Neuenheimer Feld 504, 69120 Heidelberg, Germany, and †Zentrum für Molekularbiologie der Universität Heidelberg, Im Neuenheimer Feld 282, 69120 Heidelberg, Germany

Trypanosoma brucei, the causative agent of African sleeping sickness, encodes three nearly identical genes for cysteine-homologues of the selenocysteine-containing glutathione peroxidases. The enzymes, which are essential for the parasites, lack glutathione peroxidase activity but catalyse the trypanothione/Tpx (tryparedoxin)-dependent reduction of hydroperoxides. Cys^{47}, Gln^{82} and Trp^{137} correspond to the selenocysteine, glutamine and tryptophan catalytic triad of the mammalian selenoenzymes. Site-directed mutagenesis revealed that Cys^{47} and Gln^{82} are essential. A glycine mutant of Trp^{137} had 13 % of wild-type activity, which suggests that the aromatic residue may play a structural role but is not directly involved in catalysis. Cys^{95}, which is conserved in related yeast and plant proteins but not in the mammalian selenoenzymes, proved to be essential as well. In contrast, replacement of the highly conserved Cys^{76} by a serine residue resulted in a fully active enzyme species and its role remains unknown. Thr^{50}, proposed to stabilize the thiolate anion at Cys^{47}, is also not essential for catalysis. Treatment of the C76S/C95S but not of the C47S/C76S double mutant with H_2O_2 induced formation of a sulfinic acid and covalent homodimers in accordance with Cys^{47} being the peroxidative active site thiol. In the wild-type peroxidase, these oxidations are prevented by formation of an intramolecular disulfide bridge between Cys^{47} and Cys^{95}. As shown by MS, regeneration of the reduced enzyme by Tpx involves a transient mixed disulfide between Cys^{95} of the peroxidase and Cys^{40} of Tpx. The catalytic mechanism of the Tpx peroxidase resembles that of atypical 2-Cys-peroxiredoxins but is distinct from that of the selenoenzymes.

Key words: enzyme catalysis, glutathione peroxidase-type tryparedoxin peroxidase, peroxiredoxin, thiol metabolism, *Trypanosoma brucei*, trypanothione.

INTRODUCTION

Trypanosomatids are the causative agents of African sleeping sickness (*Trypanosoma brucei gambiense* and *Trypanosoma brucei rhodesiense*), Nagana cattle disease (*Trypanosoma congolense* and *Trypanosoma brucei brucei*), South American Chagas' disease (*Trypanosoma cruzi*) as well as the different forms of leishmaniasis (*Leishmania* species). Trypanosomes and leishmania differ from all other known eukaryotes and prokaryotes in their unique thiol redox metabolism. The thiol–polyamine conjugate trypanothione [N^1,N^8-bis(glutathionyl) spermidine] and the flavoenzyme trypanothione reductase replace the nearly ubiquitous glutathione/glutathione reductase system [1,2].

In the mammalian host, trypanosomes are exposed to various reactive oxygen species but their ability to cope with oxidative stress is rather weak. The parasites lack catalase and selenocysteine-containing glutathione peroxidases but have 2-Cys-peroxiredoxins [3–5] and cysteine-homologues of the classical glutathione peroxidases [6–8]. Both types of peroxidases obtain their reducing equivalents from the dithiol protein Tpx (tryparedoxin) [9,10]. With NADPH as final electron donor, the reducing equivalents flow via trypanothione on to Tpx and from this on to the peroxidases that catalyse the reduction of the hydroperoxide [3–9]. Thus the 2-Cys-peroxiredoxins and the glutathione peroxidase-type enzymes in these parasites act as trypanothione-dependent Tpx peroxidases. In *T. brucei*, both types of peroxidases occur in the cytosol and mitochondrion [4,8]. RNA interference studies revealed that the cytosolic 2-Cys-peroxiredoxin and the glutathione peroxidase-type enzymes are essential [8,11].

Four types of GPXs (selenocysteine-containing glutathione peroxidases) have been characterized in mammals, namely the cytosolic glutathione peroxidase, cGPX (GPX-1, also called classical or cellular glutathione peroxidase), the gastrointestinal glutathione peroxidase, GI-GPX (GPX-2), the extracellular glutathione peroxidase, pGPX (GPX-3), found in human plasma, and the phospholipid hydroperoxide glutathione peroxidase, PhGPX (GPX-4), but probably only GPX-1 functions in oxidative defence [12]. Genes encoding cysteine-homologues of glutathione peroxidases are widespread in nature but only few of the enzymes have been characterized. Site-directed mutagenesis of the mammalian phospholipid hydroperoxide glutathione peroxidase revealed that a catalytic triad composed of $SeCys^{46}$, Gln^{81} and Trp^{136} is involved in catalysis and it was suggested that different or additional amino acid residues are important in cysteine-homologues [13]. In the thioredoxin-dependent cysteine-containing glutathione peroxidases of Chinese cabbage and *Saccharomyces cerevisiae* an intramolecular disulfide bond was shown to be an essential catalytic intermediate [14–16]. The residues involved are the proposed active site cysteine and a cysteine that is not conserved in the selenoenzymes (Figure 1) [14,15,17].

T. brucei has a genomic locus that encodes three genes for cysteine-containing glutathione peroxidases [Px I–III, where Px is glutathione peroxidase-type Tpx peroxidase (cysteine-homologue of glutathione peroxidases)]. The activity of recombinant Px III

Abbreviations used: CM, carboxamidomethyl; DTE, dithioerythritol; DTNB, 5,5′-dithiobis-(2-nitrobenzoic acid); DTT, dithiothreitol; ESI–MS, electrospray ionization MS; GPX, selenocysteine-containing glutathione peroxidase; IAM, iodoacetamide; MALDI–TOF-MS, matrix-assisted laser-desorption ionization–time-of-flight MS; Ni-NTA, Ni^{2+}-nitrilotriacetate; Tpx, tryparedoxin; Px, glutathione peroxidase-type Tpx peroxidase (cysteine-homologue of glutathione peroxidases); TFA, trifluoroacetic acid; TS_2, trypanothione disulfide.

[1] To whom correspondence should be addressed (email luise.krauth-siegel@bzh.uni-heidelberg.de).

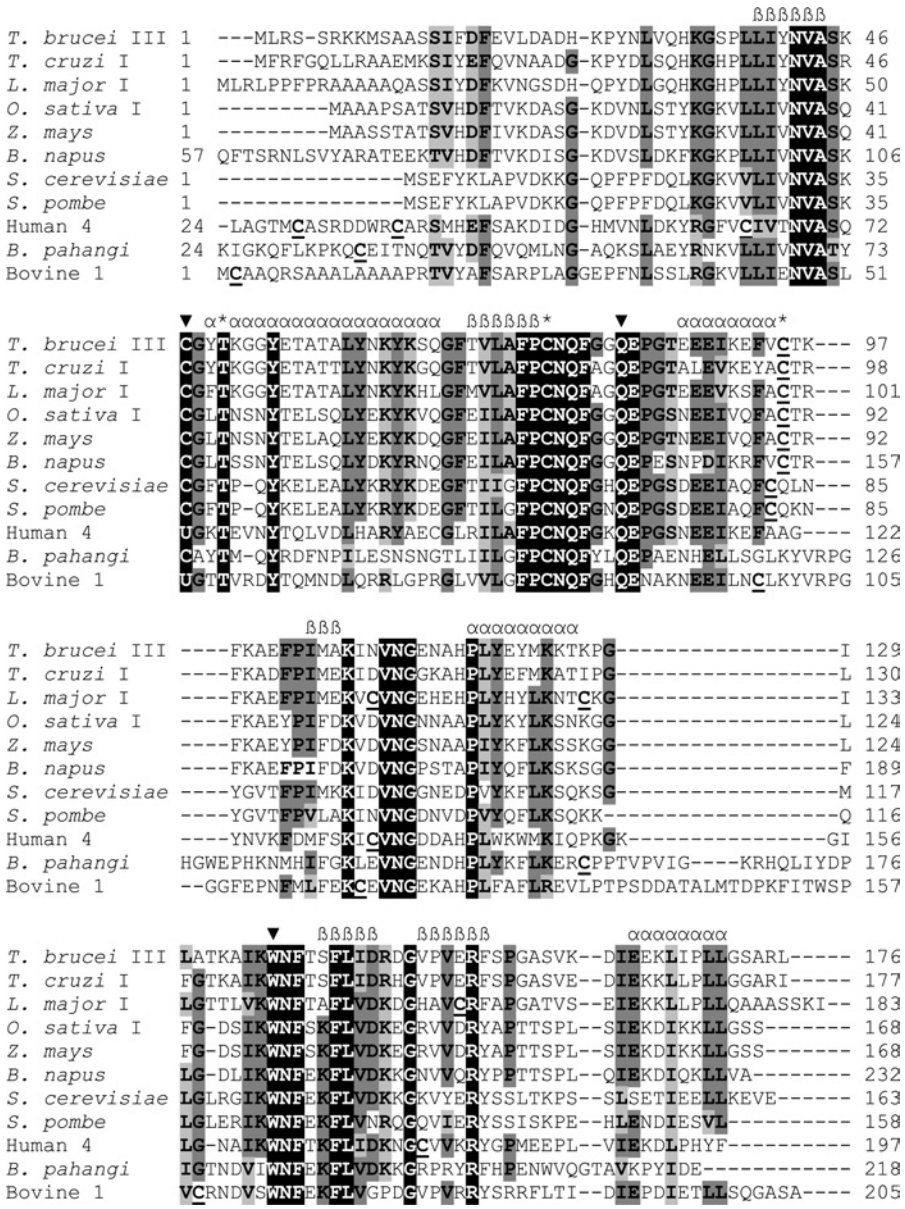

Figure 1 Comparison of *T. brucei* Px III with other proteins

The residues U (SeCys) or C, Q and W that form the catalytic triad of glutathione peroxidases are marked by triangles. The α-helical (α) and β-sheet (β) regions above the alignment refer to secondary structure elements in the crystal structure of bovine GPX-1 [24]. Residues that are identical in all or at least eight of the 11 sequences are depicted in white on a black background and in bold on dark grey respectively. Residues that are similar in at least eight sequences are shown in bold on light grey. Other Cysteine residues are given in bold letters and underlined. Residues that, in addition to the catalytic triad, were mutated in the *T. brucei* Px III are marked by an asterisk. *T. brucei* III, *T. brucei* Px III (no. CAC83349.1); *T. cruzi* I, *T. cruzi* glutathione peroxidase-type enzyme I (no. CAC85914); *L. major* I, *Leishmania major* putative glutathione peroxidase-like protein 1 (no. CAJ04920); *O. sativa* I, *Oryza sativa* glutathione peroxidase 1 (no. AAM47493.1); *Z. mays*, *Zea mays* putative glutathione peroxidase (no. AAT42154.1); *B. napus*, *Brassica napus* (Chinese cabbage) glutathione peroxidase (no. AAM12502.1); *S. cerevisiae*, *Saccharyomyces cerevisiae* thiol peroxidase Hyr1p [(PH)Gpx3, no. NP_012303]; Human 4, human GPX-4 (no. CAA50793); *B. pahangi*, *Brugia pahangi* glutathione peroxidase (no. CAA48882); Bovine 1, cytosolic glutathione peroxidase from bovine erythrocytes (GPX-1, no. P00435).

is five orders of magnitude higher with the trypanothione/Tpx system when compared with GSH [7]. Possible physiological substrates are H_2O_2, thymine hydroperoxide and linoleic acid hydroperoxide. Phosphatidylcholine hydroperoxide is not reduced but even inhibits the enzyme [8]. Here, we report on the catalytic mechanism of recombinant *T. brucei* Px III as revealed by site-directed mutagenesis. The mechanism of the Tpx-dependent Px III resembles that of atypical 2-Cys-peroxiredoxins and clearly contrasts with that of the GPX.

EXPERIMENTAL

Materials

Recombinant His_6–Px III [7], *T. brucei* Tpx [18] and *T. cruzi* trypanothione reductase [19] were prepared as described. Polyclonal rabbit antibodies against His_6–Px III [7] and *T. brucei* Tpx [20] were produced by Bioscience (Göttingen, Germany) and Eurogentec respectively. The BL21 (DE3) *Escherichia coli* strains expressing the C40S and C43S mutants of *T. brucei* Tpx–His_6

Table 1 Mutagenesis primer

f, forward; r, reverse

Px III species	Primer	Sequence	Mutation
C47S	1f	caatgtggcaagtaaaTCCggttacacaaagggtgg	TGC/TCC
	1r	ccacccttgtgtaaccGGAtttacttgccacattg	GCA/GGA
C76S	2f	gttctggcgttcccgTCTaaccaatttggtgg	TGT/TCT
	2r	ccaccaaattggttAGAcgggaacgccagaac	ACA/AGA
C95S	3f	ggaaatcaaggagtttgtaTCCaccaagttcaaggc	TGC/TCC
	3r	gccttgaacttggtGGAtacaaactccttgatttcc	GCA/GGA
Q82G	PXQG1f	gtgtaaccaatttggtggtGGGgaacccggaaacg	CAG/GGG
	PXQG1r	cgtttccgggttcCCCaccaccaaattggttacac	CTG/CCC
W137G	PXWG1f	gcaacgaaggctatcaaaGGGaactttacatccttcc	TGG/GGG
	PXWG1r	ggaaggatgtaaagttCCCtttgatagccttcgttgc	CCA/CCC
T50S	T50Sf	caatgtggcaagtaaatgcggttacTCAaagggtgg	ACA/TCA
	T50Sr	ccaccctTGAgtaaccgcatttacttgccacattg	TGT/TGA
T50V	T50Vf	gatatacaatgtggcaagtaaatgcggttacGTAaagggtgg	ACA/GTA
	T50Vr	ccaccctTACgtaaccgcatttacttgccacattgtatatc	TGT/TAC

were a gift from Dr Leopold Flohé (MOLISA GmbH, Magdeburg, Germany). TS_2 (trypanothione disulfide) was purchased from Bachem and H_2O_2 from Merck. All other chemicals were of the highest purity available.

Cloning, heterologous expression and purification of Px III mutants

Site-directed mutageneses were performed using the QuikChange® Site-directed Mutagenesis kit (Stratagene). A pQE30 vector with the His_6–Px III wild-type gene [7] served as a template to generate the single mutants by PCR using the primers given in Table 1. Double mutants were obtained with the same primers and a pQE30 vector that already contained a single mutation. Annealing and synthesis were performed at 55 °C for 1 min and at 68 °C for 5 min respectively. The cycle number was 12 in the case of the C47S, C76S, C95S, C47S/C76S, C76S/C95S, C47S/C95S and W137G mutants and 16 for generating the Q82G, T50S and T50V variants. The methylated original plasmid was removed by digestion with *Dpn*I. *Escherichia Coli* XL1-Blue cells were transformed and grown at 37 °C in LB (Luria–Bertani) medium containing 100 μg/ml carbenicillin. DNA was extracted by the Nucleobond® PC100 kit (Macherey-Nagel) and the purified plasmids were sequenced (MWG-Biotech). The recombinant wild-type and mutant Px III species were prepared essentially as described in [7]. Protein concentrations were obtained from absorption measurements at 280 nm. For the pure wild-type Px III and the C47S, C76S, C95S, Q82G, T50S, T50V, C47S/C76S, and C76S/C95S mutants, an A_{280} (absorbance) of 1 corresponds to 1 mg/ml. For the W137G mutant an A_{280} of 1 corresponds to 1.69 mg/ml. The proteins were stored at 4 °C.

Preparation of the C40S and C43S mutants of *T. brucei* Tpx

The *T. brucei* Tpx mutants were prepared following a slightly modified protocol of Budde et al. [21]. The protein concentration was estimated at A_{280} by using the factor for tag-free wild-type Tpx [18] where an A_{280} of 1.7 corresponds to 1 mg/ml protein. The proteins were stored at 4 °C.

Peroxidase standard assay

The trypanothione/Tpx-dependent peroxidase activity of wild-type and mutant Px III was followed at 25 °C in a total volume of 150 μl of 0.1 M Tris/HCl and 5 mM EDTA (pH 7.6), containing 240 μM NADPH, 100 μM TS_2, 150 m-units of *T. cruzi* trypanothione reductase, 10 μM wild-type *T. brucei* Tpx, and 0.13–2 μM of the different Px III species. The reaction was started by adding 100 μM H_2O_2, and NADPH oxidation was followed at 340 nm. The total concentration of hydroperoxide in the assay was determined by allowing the reaction with wild-type Px III to run to completion. The consumption of NADPH in the presence of all assay components except Px III was subtracted. The pH optimum of Px III was determined in 50 mM Tris/HCl, 50 mM Mes, 1 mM EDTA and 0.5 mg/ml BSA between pH 6.5 and 9.0. The composition of the reaction mixtures was that of the standard assay. The conductivity of the buffers varied only between 1.7 and 2.5 mS excluding that the activities at different pH values are caused by changes in ionic strength.

Determination of thiol groups

The concentration of thiol groups was determined with DTNB [5,5′-dithiobis-(2-nitrobenzoic acid); ε_{412} (molar absorption coefficient) = 13.6 $mM^{-1} \cdot cm^{-1}$] [22]. The reaction mixtures contained 200 μM DTNB and 10–100 μM thiol in 50 mM potassium phosphate (pH 8.0). The total thiol groups of the Px III species were determined directly after elution of the proteins from the Ni-NTA (Ni^{2+}-nitrilotriacetate) column and after treatment with excess thiols. For this purpose, 50 μM of Px III in 50 mM sodium phosphate, 300 mM NaCl and 250 mM imidazole (pH 8.0) was incubated with 150 mM 2-mercaptoethanol overnight at 4 °C. Excess 2-mercaptoethanol was removed and the buffer was exchanged against 100 mM Tris/HCl and 1 mM EDTA (pH 8.0) in an Amicon 10K concentrator (Millipore). In the samples not treated with thiols, the imidazole-containing buffer was exchanged by the same procedure. Freshly prepared C40S and C43S Tpx mutants (50 μM) were incubated with 1 mM 2-mercaptoethanol and treated accordingly.

Western blot analysis of the mixed disulfide between Px III and Tpx

Stock solutions (50 μM) of the different Px III and Tpx species were obtained in 50 mM sodium phosphate and 300 mM NaCl (pH 8.0) containing 250 or 150 mM imidazole. In a total volume of 28 μl adjusted with water, 3.3 μM wild-type or C76S Px III was incubated for 1 min at room temperature (25 °C) with 7.9 μM of reduced *T. brucei* C40S or C43S Tpx respectively. A control contained in addition 1 mM 2-mercaptoethanol. In a second series, the Px III species were mixed with the Tpx mutant; after 1 min at room temperature, 300 μM H_2O_2 was added and the reaction mixtures were incubated for a further 1 min. To assess the possible formation of homodimers under these conditions, the Px III and Tpx species were individually treated with 300 μM H_2O_2 or 1 mM 2-mercaptoethanol or an equal volume of water. In the case of oxidized samples, the reactions were stopped by adding 1/4 vol. of 4× sample buffer [250 mM Tris, pH 6.8, 8 % (w/v) SDS, 40 % (v/v) glycerol and 0.004 % (w/v) Bromophenol Blue]. In the case of reduced proteins, the sample buffer contained 100 mM DTE (dithioerythritol). The samples were boiled for 5 min and 12 μl of the reaction mixture was loaded on to an SDS/10 % polyacrylamide gel. After electrophoresis, the proteins were transferred on to a Hybond™-P membrane (Amersham Biosciences) by wet electroblotting and probed with the polyclonal rabbit antiserum against Px III (1:1000) and Tpx (1:1000) respectively. Horseradish peroxidase-conjugated anti-rabbit IgG (1:20 000; Santa Cruz Biotechnology) served as the secondary antibody. The immune complexes were visualized by the SuperSignal® West Pico chemiluminescent substrate (Pierce).

ESI–MS (electrospray ionization mass spectrometry) analysis of Px III

Wild-type or C76S Px III (50 μM) in 50 mM sodium phosphate, 300 mM NaCl and 250 mM imidazole (pH 7.6) was treated at room temperature either for 20 min with 15 mM IAM (iodoacetamide) or first for 20 min with 2 mM DTT (dithiothreitol) followed by 20 min with 19 mM IAM. Water was added to give a final concentration of 10 μM protein and 100 μl of the sample was injected into the HPLC system (Agilent Technologies) online coupled with an API-QSTAR™ Pulsar instrument (Applied Biosystems). The protein was trapped on a 50 Poros R1 trapping column. After 1.5 min of washing [0.1 % TFA (trifluoroacetic acid); 0.4 ml/min], the protein was eluted into the electrospray ion source with 80 % (v/v) acetonitrile and 0.1 % TFA at 20 μl/min essentially as described by Rist et al. [23]. The ESI–Q-TOF (quadrupole–time-of-flight) instrument was calibrated with apomyoglobin (Sigma) resulting in a mass accuracy better than 100 p.p.m. C76S/C95S and C47S/C76S Px III (50 μM) in 50 mM sodium phosphate, 300 mM NaCl and 250 mM imidazole (pH 7.6) were incubated overnight with 150 mM 2-mercaptoethanol at 4 °C. The reducing agent was removed by gel filtration on a PD10 column (Amersham Biosciences) equilibrated in 100 mM Tris/HCl and 1 mM EDTA (pH 7.6). In a total volume of 240 μl, 6 or 8 μM of reduced Px III was incubated with an equimolar concentration of H_2O_2 for 8 min at room temperature. The reaction was stopped by adding catalase and the protein solution was kept on ice until it was analysed by ESI–MS.

MALDI–TOF-MS (matrix-assisted laser-desorption ionization–time-of-flight MS) analysis of the intermolecular disulfide between C76S Px III and C43S Tpx

Three microlitres of 50 μM C76S Px III (directly after elution from the Ni-NTA column) and 6 μl of 50 μM reduced C43S Tpx (see above) were mixed with 6 μl of water to give final protein concentrations of 10 and 20 μM respectively. After 1 min at room temperature, IAM was added to a final concentration of 10 mM. After 20 min, the protein mixture was digested with GluC and subsequently with trypsin (2 h at 37 °C each) at a protein/protease ratio of 10:1 (w/w). An aliquot of the solution was treated with 30 mM DTT for 20 min to generate the cysteine-containing peptides in free form. Peptides were analysed by MALDI–TOF-MS on a Bruker Ultraflex mass spectrometer. The peptide solution in 50 mM ammonium bicarbonate/HCl (pH 7.5) was desalted on a ZipTip μC18 column (Millipore). The MALDI-Matrix was prepared as a saturated solution of α-cyano-4-hydroxycinnamic acid in acetonitrile and 0.1 % TFA (1:1, v/v). A nitrogen laser (337 nm) was employed for desorption/ionization, and the ion acceleration voltage was 20 kV. The spectra from 400 laser shots were averaged. The instrument was calibrated externally with peptide standard II from Bruker, resulting in a mass accuracy of 100 p.p.m. For peptide sequencing by MALDI–TOF–TOF-MS, peptide fragments were generated by post source decay and fragment spectra were acquired on a Bruker Ultraflex mass spectrometer using the LIFT method. The precursor mass window was 1 % of the mass of the parent ion.

Modelling of the three-dimensional structure of Px III

Blasting the sequence of *T. brucei* Px III against the SWISS-MODEL PDB revealed human GPX-4 (PDB entry 2GS3) and bovine erythrocytes GPX-1 (PDB entry 1GP1) [24] suited as template structures with a Poisson unlikelihood probability $P(N)$ score [25] of 3×10^{-30} and 3×10^{-19} respectively. *T. brucei* Px III lacks 18 residues in its C-terminal moiety, which in the tetrameric GPX-1 are involved in subunit interactions (see Figure 1). To fit the structure of the *T. brucei* Px III from Gly^{128} onwards, the stretch Pro^{139} to Ser^{156} of the bovine enzyme was artificially introduced between Gly^{128} and Ile^{129}. This allowed the generation of a model comprising also the C-terminal region of the parasite Px III. The second model was obtained using the recent crystal structure of the monomeric human GPX-4 as a template. Details of the procedure are described in the literature [26]. The three-dimensional structures were visualized and analysed with the program Swiss-PdbViewer [27].

RESULTS AND DISCUSSION

The *T. brucei* glutathione peroxidase-type Tpx peroxidases have three conserved cysteine residues

T. brucei encodes three nearly identical genes for cysteine homologues of the GPX [7]. The parasite proteins (Px I–III) show an overall sequence identity of 52 and 45 % with glutathione peroxidase-type peroxidases from *Oryza sativa* and Chinese cabbage respectively. Of the mammalian selenoproteins, GPX-4 is the closest relative that shares 39 % of all residues and is also monomeric. The parasite peroxidases contain three conserved cysteine residues (Figure 1). Cys^{47} in Px III, which replaces the selenocysteine of classical glutathione peroxidases, forms the active site. Cys^{76} occurs in almost all glutathione peroxidases and is embedded in a strictly conserved stretch of FPCNQF. In addition, the trypanosomatid peroxidases as well as related proteins from yeast, fungi and plants possess a third cysteine residue that corresponds to Cys^{95} of the *T. brucei* Px III [7,14,17]. Cys^{95} is part of an F(Y), A(V), CT consensus motif that may facilitate the interaction with the dithiol proteins acting as reducing substrates. This cysteine is not conserved in the selenoenzymes as well as in several cysteine-homologues (Figure 1) [28].

Cys^{47}, Gln^{82} and Cys^{95} are essential for peroxidase activity

Gln^{82} and Trp^{137} were replaced by glycine and the three cysteine residues Cys^{47}, Cys^{76} and Cys^{95} were replaced by serine. Because the enzyme does not show classical saturation kinetics [7], kinetic constants were not determined but the initial ΔA/min-values at fixed concentrations of trypanothione, trypanothione reductase, Tpx and H_2O_2 were compared. Cys^{47}, Gln^{82} and Cys^{95} proved to be essential; an exchange of any of these residues abolished the peroxidase activity (Table 2). The absolute requirement for two cysteine residues has also been shown for glutathione peroxidase-type enzymes from yeast [14] and Chinese cabbage [15]. These proteins as well as a peroxidase from *Plasmodium falciparum* obtain their reducing equivalents preferably from thioredoxin. GSH is a poor or no substrate at all [7,14–16,29]. In the Chinese cabbage peroxidase, replacement of Gln^{142} by a glycine did not affect the activity towards H_2O_2 [15]. This contrasts with our results on *T. brucei* Px III as well as with data for the mammalian GPX-4 [13]. In both enzymes, replacement of this glutamine dramatically lowered the peroxidase activity. Replacement of Trp^{137} by a glycine yielded a Px III species with 13 % of wild-type activity. The low but significant activity of the mutant indicates that the conserved tryptophan may play a structural role but is not directly involved in catalysis.

C76S Px III showed wild-type activity. Cys^{76} is conserved in both the selenoenzymes and in the cysteine-containing enzymes and occupies a prominent position at the C-terminal end of the

Table 2 Specific activity and thiol content of wild-type and mutant Px III species

Enzyme activities were determined with H_2O_2 as substrate.

		Px III species							
		Wild-type	C47S	C76S	C95S	Q82G	W137G	T50S	T50V
	Activity (%)*	100	0 ± 0	104 ± 8.2	1.8 ± 3.1	2.4 ± 0.3	12.9 ± 1.8	79 ± 9.0	39 ± 2.0
Cysteine residues	Theoretical	3	2	2	2	3	3	3	3
reacting with	Without pre-reduction†	0.6 ± 0.2	1.0	0.2 ± 0.1	0.7	0.7	1.0	0.6 ± 0.2	0.7 ± 0.3
DTNB	After pre-reduction‡	1.6 ± 0.3	1.6 ± 0.3	0.9 ± 0.2	1.1 ± 0.1	1.1–1.8	1.5–1.6	1.1–1.4	1.1–1.4

* The activity (%) of the mutants refers to wild-type enzyme prepared in parallel. Results are means ± S.D. for at least three independent measurements.
† The values for the oxidized protein samples represent either single measurements or, when standard deviations are given, are the means for at least three independent measurements.
‡ The values for the reduced samples are the averages of at least two independent measurements.

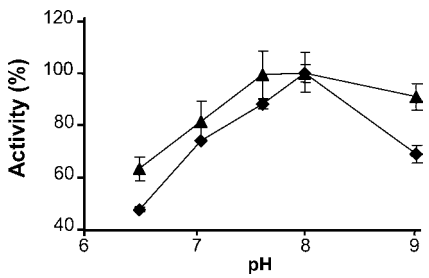

Figure 2 pH profile of wild-type and C76S Px III

The activities of wild-type (▲) and C76S (◆) Px III were measured in 50 mM Tris/HCl, 50 mM Mes and 1 mM EDTA between pH 6.5 and 9.0. The assays contained 100 μM trypanothione, 10 μM Tpx, 0.5 mg/ml BSA and 100 μM hydroperoxide substrate as described under the Experimental section. Results are means ± S.D. for at least three measurements.

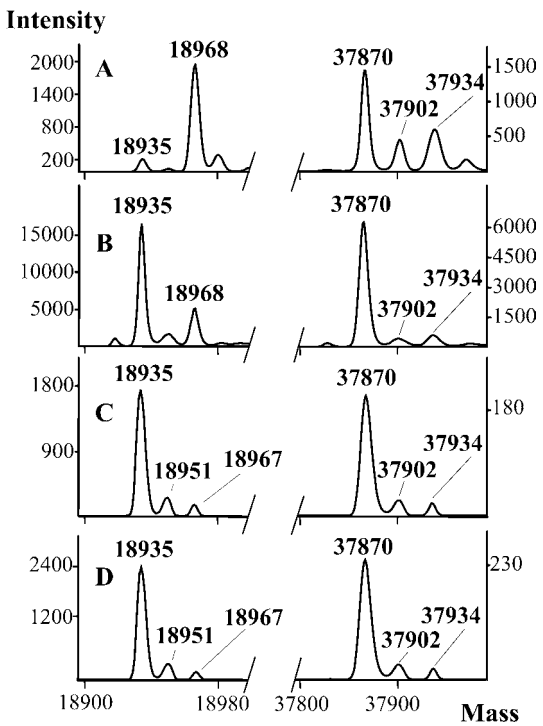

Figure 3 Deconvoluted ESI–MS spectra of Px III double mutants treated with H_2O_2

(**A**) Reduced C76S/C95S Px III was incubated with an equimolar concentration of H_2O_2 as described under the Experimental section. The peak at 18935 Da corresponds to the theoretical mass of the tag-free unmodified protein. The masses of 18968 and 37870 Da are in accordance with the incorporation of two oxygen atoms and formation of a covalent dimer respectively. (**B**) Untreated sample of C76S/C95S Px III stored at 4 °C. (**C**) Reduced C47S/C76S Px III treated with H_2O_2. (**D**) Untreated C47S/C76S Px III. The spectra shown in (**C**, **D**) are practically identical. The main peaks at 18935 and 37870 Da correspond to the monomeric (calculated mass 18935 Da) and dimeric (calculated mass 37868 Da) forms of the protein respectively. The additional peaks with 16, 32, and 64 Da higher masses that accompany the main peaks are probably oxidation products.

second β-sheet (Figure 1). The residue probably plays a functional or regulatory role, although this has not yet been elucidated. In the Chinese cabbage enzyme, the respective C136S mutation lowered the activity by 70 %. In this protein, Cys^{155} (corresponding to Cys^{95} in Px III) can also form an intramolecular disulfide bridge with Cys^{136} (corresponding to Cys^{76} in Px III) and the possibility was discussed that there may be a disulfide bond exchange between three cysteine residues and/or that Cys^{136} plays a structural role [15]. For the *T. brucei* enzyme, a three-cysteine mechanism is very unlikely because the C76S variant of Px III had wild-type activity against H_2O_2. Wild-type and C76S Px III showed a pH optimum of 8.0. The profiles were rather flat and, at pH 6.5, the wild-type enzyme had still 65 % of the maximum activity (Figure 2). In comparison, pig heart GPX-4 and a mutant with a cysteine replacing the selenocysteine [13] as well as the cysteine-containing glutathione peroxidase from the nematode *Brugia pahangi* [30] have slightly higher pH optima at 8.2 and 8.5 respectively and show only minute activity at pH 6.5. The pH profiles of the different peroxidases probably reflect mainly the dissociation of their thiol substrates. The p*K* value of *T. brucei* Tpx is 7.2 [20], whereas that of GSH is 8.7.

Cys^{95} is also essential for Px III. The lack of peroxidase activity of the C76S/C95S double mutant is not due to overoxidation or dimerization of the protein. Even after long-range storage, Px III occurred predominantly as monomer with a thiol group at Cys^{47} (see Figure 3B) that reacted with DTNB (results not shown). Neither wild-type Px III [7] nor the C95S mutant (results not shown) had significant peroxidase activity with GSH. Thus, in the absence of Cys^{95}, when the intramolecular disulfide bond between Cys^{47} and Cys^{95} cannot be formed (see below), Px III does not adopt the mechanism of the classical selenoenzymes. Recently, a thioredoxin-dependent glutathione peroxidase-type enzyme from *Drosophila melanogaster* has been characterized. The protein forms also an intramolecular disulfide, namely between Cys^{45} and Cys^{91}; the latter cysteine residue does not align with Cys^{95} of Px III but occupies position 92 of the parasite protein. Interestingly, in the insect enzyme, replacement of Cys^{91} increased the low rate constant for the reduction of the wild-type peroxidase by GSH 3-fold [28]. It should be noted that not all cysteine-containing glutathione peroxidase-type enzymes are monomeric and use

dithiol proteins as electron source. The nematode *B. pahangi* has been reported to secrete a glutathione peroxidase-type enzyme. The enzyme is tetrameric and under *in vitro* conditions catalyses the glutathione-dependent reduction of a variety of hydroperoxides but not of H_2O_2 [30].

The thorough structural analysis of (di)thiol redox proteins aligned the CXXT motif of glutathione peroxidases with the CXXC motif of thioredoxins and the threonine was proposed to stabilize the catalytic thiolate by hydrogen-bonding [17]. The mutational analysis of the *T. brucei* Px III is the first study to (dis)prove this hypothesis. Replacement of Thr^{50} by serine or valine resulted in enzyme species with approx. 80 and 40 % remaining activity. Thus the threonine residue is not essential for catalysis but a residue that is able to form a hydrogen bond may stabilize the active-site structure. The model of Px III (see below) also did not reveal a direct interaction of the two side chains. Instead, hydrogen bonds may be formed between the peptide NH of Cys^{47} and the side chain oxygen of Thr^{50} as well as between the main chain NH of Thr^{50} and the carbonyl oxygen of Cys^{47}. Also in the crystal structure of the bovine enzyme a direct interaction between the side chains of the $SeCys^{52}$ and Thr^{55} is not evident.

Cys^{47} is the peroxidative cysteine that in the absence of Cys^{95} is oxidized to a sulfinic acid

In freshly prepared wild-type and C76S Px III, 0.6 and almost no thiol group respectively reacted with DTNB (Table 2) in accordance with Cys^{76} being the residue that reacted in the wild-type enzyme. The Px III mutants with Cys^{47}, Cys^{95}, Gln^{82}, Trp^{137} or Thr^{50} exchanged also did not reveal the theoretical number of thiols per protein molecule. After pre-reduction, C47S Px III – but not the C76S, C95S and other mutants – yielded the expected number of thiol groups per protein molecule. Obviously, Cys^{47} rapidly reoxidizes, preventing reaction with DTNB. The ESI–MS analysis of the C76S/C95S and C47S/C76S double mutants corroborated this interpretation. Treatment of C76S/C95S Px III with an equimolar concentration of H_2O_2 led to a peak with a mass of 18 968 Da (calculated mass 18 967 Da) that was 32 Da higher than that of the untreated protein (observed and calculated mass 18 935 Da). In addition, a peak at 37 870 Da was in accordance with formation of the homodimer (calculated mass 37 868 Da; Figure 3A). Most probably the peak at 18 968 Da represents the Px III mutant with a cysteine sulfinic acid at position 47. Also storage of this mutant under aerobic conditions generated some oxidized protein species (Figure 3B). In contrast, the total mass determination of the C47S/C76S double mutant revealed mainly unmodified monomer (18 935 Da), independent of H_2O_2 treatment or storage (Figures 3C and 3D). Thus Cys^{47} is the reactive active site thiol that rapidly oxidizes to a sulfinic acid if Cys^{95} is lacking.

Cys^{47} and Cys^{95} form an intramolecular disulfide bridge

In wild-type and C76S Px III, Cys^{47} and Cys^{95} can form an intramolecular disulfide bridge. Formation of intermolecular disulfides is not significant. Wild-type Px III eluted from the gel chromatography column as a monomer [7] and SDS/PAGE under non-reducing conditions (Figure 4A, lane a) showed mainly monomeric protein. Wild-type and C76S Px III were alkylated with IAM in the absence or presence of DTE and subjected to ESI–MS analysis (Table 3). The observed total masses of both untreated protein species were 2 Da lower than the calculated masses for the reduced protein species, which was a first indication that an intramolecular disulfide bridge had been formed. Treatment of the wild-type Px III, but not of the C76S mutant, with IAM

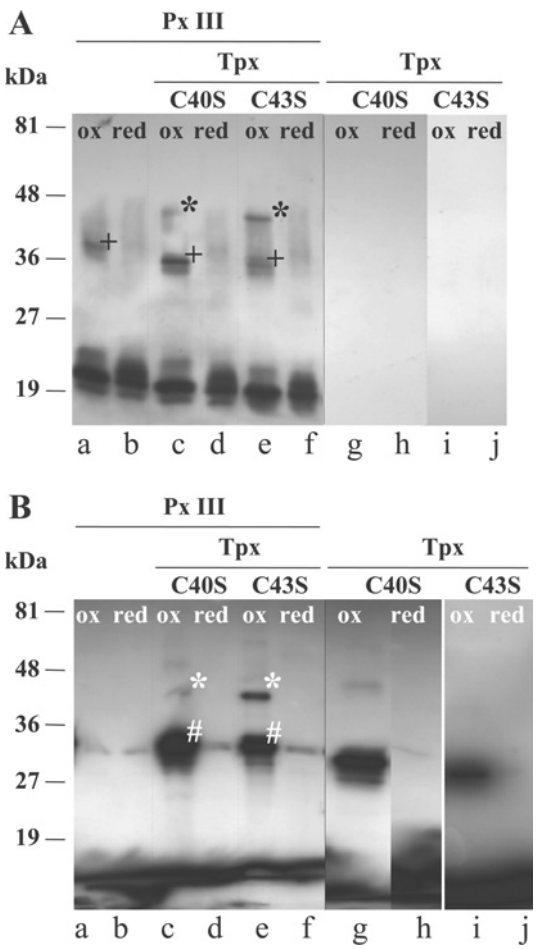

Figure 4 Western blot analysis of mixed disulfides between *T. brucei* peroxidase and Tpx

Wild-type Px III was incubated with C40S or C43S Tpx as described in the Experimental section; ox, samples without reducing agent in the sample buffer; red, protein sample treated with 1 mM 2-mercaptoethanol and boiled in sample buffer with 100 mM DTE. The blots were developed with antibodies against (**A**) Px III or (**B**) Tpx. *, Mixed disulfides between Px III and Tpx; +, Px III homodimers; #, Tpx homodimers. His_6–Px III has a molecular mass of 21 kDa. As observed previously, the recombinant protein is often cleaved between two basic residues of the RKK motif within the mitochondrial targeting signal by a co-purified bacterial protease resulting in a second band with 19 kDa [7]. The Tpx–His_6 monomers have a mass of 17 kDa but run at 14–15 kDa. The mixed protein disulfides have expected sizes of 36 or 38 kDa.

in the absence of DTE caused the incorporation of one CM (carboxamidomethyl) group. In contrast, in the presence of excess thiol, three molecules of IAM reacted with wild-type Px III and two with the C76S mutant. The results show that Cys^{47} and Cys^{95} form a disulfide bridge. This also explains why in the wild-type protein $\leqslant 1$ of the three cysteine residues reacted with DTNB (Table 2). One reason for Cys^{95} being essential is obviously the formation of the intramolecular disulfide bridge to prevent unspecific (over)oxidation of Cys^{47} upon reaction with the hydroperoxide substrate.

Px III forms a mixed disulfide with Tpx

The physiological electron donor of Px III is Tpx [7]. Most probably a mixed disulfide between Px III and one of the two active site cysteine residues of the dithiol protein is formed. Because this intermolecular disulfide is immediately attacked by the vicinal second cysteine of Tpx, stable mixed disulfides

Table 3 Disulfide bond formation between Cys[47] and Cys[95] of Px III as revealed by ESI-MS

Wild-type or C76S Px III was treated with IAM in the absence or presence of excess thiol as described under the Experimental section. Alkylation of reduced wild-type Px III caused a mass increase of 172 Da in accordance with the incorporation of three CM groups (3 × 57 Da), whereas the oxidized protein was alkylated at a single site (57 Da). As expected, the reduced C76S mutant showed the addition of two CM groups (2 × 57 Da) and the oxidized protein did not react with IAM. S-S, intramolecular disulfide. *The deconvoluted ESI–MS spectra showed the expected masses but the highest peaks corresponded to a 13 or 14 Da higher mass. This is probably due to a modification within the His tag. The spectrum of the untreated wild-type protein revealed also a peak at 18967 Da corresponding to the protein without His tag [7]. For this protein species, the observed and calculated masses were identical.

Px III species	Treatment	Mass (Da)		Cysteine modifications
		Calculated	Observed*	
Wild-type	None	20965	20979	1 × SH, 1 S-S
	2 mM DTT and 19 mM IAM	21138	21151	3 × CM
	15 mM IAM	21022	21035	1 × CM, 1 S-S
C76S	None	20949	20963	1 × S-S
	2 mM DTT and 19 mM IAM	21065	21078	2 × CM
	15 mM IAM	20949	20963	1 × S-S

can only be generated as dead-end intermediates by replacing one of the cysteine residues. The recombinant C40S and C43S Tpx mutants were treated with excess 2-mercaptoethanol. After removal of the reducing agent, DTNB measurement revealed one thiol group per protein molecule. Freshly prepared, mainly oxidized (Table 2) wild-type Px III was allowed to react with the Tpx variants and the formation of mixed disulfides was analysed by Western blotting. In the first series of blots, the membrane was treated with antibodies against Px III, stripped and developed with antibodies against Tpx. Protein bands reacting with both antibodies represented mixed disulfides (results not shown). To exclude false positive results because of incomplete stripping, in the second series two identical blots were developed with antibodies against Px III (Figure 4A) or Tpx (Figure 4B). Under non-reducing conditions, Px III (Figure 4A, lane a) and the Tpx mutants (Figure 4B, lanes g and i) ran in the SDS/PAGE as mixtures of monomeric and dimeric forms. In the presence of excess thiols, the proteins occurred, as expected, as monomers (Figures 4A, lane b and 4B, lanes h and j). Wild-type Px III reacted with C43S Tpx under formation of a mixed disulfide (Figures 4A and 4B, lanes e). In comparison, incubation with C40S Tpx resulted in a tiny amount of mixed disulfide but induced formation of Px III homodimers. Probably, a non-physiological disulfide formed between the two proteins is not stable and reacts with another Px III molecule to generate the homodimer (Figure 4A, lane c). Also C76S Px III reacted almost exclusively with C43S Tpx (results not shown). These results are in accordance with Cys[40] being the thiolate of Tpx that attacks the intramolecular disulfide of Px III. The selective reaction of the more N-terminal cysteine of Tpx is in agreement with Cys[40] being the reactive [9] and solvent-exposed cysteine of the dithiol protein [31]. Cys[40] interacts with both the low-molecular-mass dithiol (trypanothione) and the protein disulfide substrates such as 2-Cys-peroxiredoxins [32] and, as shown here, the glutathione peroxidase-type enzymes. The C47S and C95S Px III mutants, which cannot form the disulfide bridge between Cys[47] and Cys[95], reacted unspecifically with both Cys[40] and Cys[43] Tpx (results not shown). In the case of C95S Px III, this resulted in large amounts of homodimers. The formation of illegitimate disulfides upon replacement of specific cysteine residues has also been reported for other proteins such as the yeast transcription factor Yap1 [14].

Cys[40] of Tpx attacks Cys[95] of Px III

To analyse which of the cysteine residues of the intramolecular disulfide bridge of Px III is attacked by Cys[40] of Tpx, C76S Px III and C43S Tpx were mixed. Free thiol groups were alkylated to prevent any thiol/disulfide exchange and the protein mixture was digested with GluC and trypsin. MALDI–TOF-MS analysis revealed a mass of 2354.9 Da that corresponds to the 93–97 peptide of the Px III mutant (calculated mass 594 Da) and the 30–44 peptide of the Tpx mutant (calculated mass 1761 Da) connected by a disulfide bridge (Figure 5A). Upon addition of DTT, the peak at 2355 Da disappeared and the free Tpx peptide (1761 Da) was detected (Figure 5B). The identity of the peptides forming the mixed disulfide was confirmed by sequencing with MALDI–TOF-TOF-MS. A peak that would correspond to a disulfide between the Cys[47]-containing 47–51 peptide of Px III (calculated mass 571.3 Da) and the 30–44 peptide of Tpx with a calculated mass of 2329.2 Da was not observed. Taken together, these results show that Cys[40] of Tpx attacks Cys[95] of the intramolecular disulfide of Px III generating an intermolecular disulfide. *T. brucei* Px III is the second glutathione peroxidase-type enzyme for which the interaction with its dithiol protein substrate has been elucidated. The other example is a recently published enzyme from *D. melanogaster*. Here, Cys[91] forms the disulfide bridge with the active site (peroxidative) cysteine residue and is subsequently attacked by thioredoxin [28]. The residue does not correspond to Cys[95] but to position 92 of Px III. Obviously, not conserved cysteine residues in the centre of the proteins can act as so-called resolving cysteine residues.

Structural model of Px III

Three-dimensional models of the *T. brucei* Px III were constructed based on the crystal structures of bovine GPX-1 [24] and a mutant of human GPX-4 with the selenocysteine replaced by a glycine residue (PDB entry 2GS3). Because the mammalian selenoenzymes do not form an intramolecular disulfide bridge, the crystal structures served as templates for the reduced Px III with Cys[47] and Cys[95] in the thiol state. The models based on the GPX-1 and GPX-4 structures comprise Asp[22] to Gly[172] and Ser[4] to Leu[171] of the parasite enzyme respectively. The overall sequence identity of Px III and GPX-1 or GPX-4 for these regions is 33 and 42 % respectively. Estimation of the stereochemical quality of the models by the program Procheck v.3.0 [33] revealed 85–88 % of all residues of Px III in most favoured regions of the Ramachandran plot. The two models showed one major difference. Ten residues form α2-helix in bovine erythrocyte GPX-1 (Asn[92] to Tyr[101]) as well as in human GPX-4 (Asn[113] to Gly[122]). When GPX-4 was used as a template, Glu[87] to Lys[97] of Px III acquired helical conformation, which resulted in a distance of 21 Å (1 Å = 0.1 nm) between Cys[95] and Cys[47]. In contrast, the model based on GPX-1 predicted that only Glu[87] to Glu[92] of Px III form helix α2 and that Cys[95] is part of the following loop (Phe[93] to His[116]) with a distance of 9.5 Å to Cys[47] (Figure 6). Preliminary NMR structural data of oxidized *T. brucei* Px III suggest that the region between Glu[87] and Lys[97] indeed lacks a pronounced secondary structure (J. Melchers and C. Muhle-Goll, unpublished work). Thus, although *T. brucei* Px III is more similar to GPX-4 with respect to the primary structure and subunit composition, the GPX-1-based model reflects the putative three-dimensional structure of Px III probably better. As shown here (Figure 5; Tables 2 and 3), Cys[47] and Cys[95] can form an intramolecular disulfide. Thus either a large conformational change accompanies each catalytic cycle or the structure of the Cys[95]-containing region differs significantly from that in the mammalian peroxidases. As expected, the

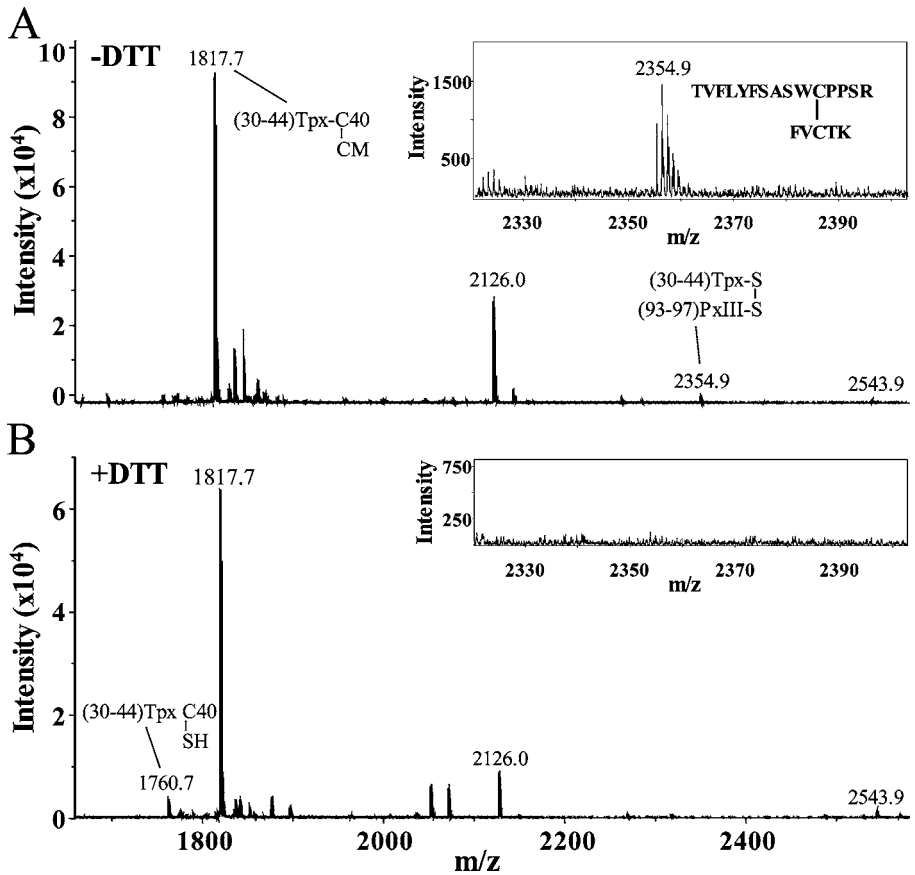

Figure 5 MALDI–TOF-MS analysis of the intramolecular disulfide bridge between Cys^{40} of Tpx and Cys^{95} of Px III

Oxidized C76S Px III was incubated with C43S Tpx, alkylated, digested with trypsin and GluC and subjected to MALDI–TOF-MS analysis as described in the Experimental section. The masses given are those of the single charged peptide ions. (**A**) The peak at 1817.7 Da reflects the CM 30–44 peptide of C43S Tpx. The peak at 2354.9 Da corresponds to a disulfide that links the 93–97 peptide of C76S Px III and the Cys^{40}-containing 30–44 peptide of C43S Tpx (expected mass 2355.1 Da). Inset: expanded region and sequence of the mixed disulfide. A peak with a mass of 2329.2 Da that would correspond to the Cys^{47}-containing 47–51 (CGYTK) peptide of Px III linked to the 30–44 peptide of C43S Tpx was not detectable. (**B**) Addition of DTT to the proteolytic digest led to the disappearance of the disulfide and the appearance of a mass at 1760.7 Da that represents the free Tpx peptide (expected mass 1760.9 Da). The origin of the peak at 2126 Da is not known.

models showed the highest atomic temperature factors for the regions around Cys^{47} and Cys^{95}. A three-dimensional structure for a cysteine-homologous glutathione peroxidase is not yet available but the crystal structures of three atypical 2-Cys-peroxiredoxins (which also form an intramolecular disulfide bridge) have been solved [34–36]. In the structure of reduced human peroxiredoxin V, the peroxidative and resolving cysteine residues are separated by 13.8 Å. It was suggested that atypical 2-Cys-peroxiredoxins employ local conformational changes of both loops that contain the peroxidative and the resolving respectively cysteine residues to change their redox states during catalysis. It is tempting to speculate that disulfide bond formation in the glutathione peroxidase-type enzymes resembles that in atypical 2-Cys-peroxiredoxins. A remote phylogenetic relationship even led to the classification of the non-selenocysteine-type glutathione peroxidases as a family of atypical 2-Cys-peroxiredoxins [16].

Proposed catalytic mechanism of Px III

Based on the mutational analysis described here, the following catalytic mechanism is proposed (Figure 7). Reduced Px III, with Cys^{47} and Cys^{95} in the thiol state, reacts with the hydroperoxide substrate, and Cys^{47} is oxidized to a sulfenic acid. It is commonly proposed for classical glutathione peroxidases that a selenate or in case of the cysteine homologues a sulfenate is the first product of catalysis but the highly reactive intermediate has not yet been directly shown [14,15,37]. The assumption that a sulfenic acid is also formed in the initial step of the reaction between Px III and the hydroperoxide substrate is based on the analogous reaction in bacterial 2-Cys-peroxiredoxins [38] and the human 1-Cys-peroxiredoxin hORF6 [39] as well as on the fact that the C76S/C95S double mutant rapidly forms a sulfinic acid when reacting with H_2O_2. In the second step of catalysis, Cys^{95} reacts with the sulfenate at Cys^{47} to form an intramolecular disulfide bridge. In the third step, Cys^{40} of Tpx attacks Cys^{95} of the Px III disulfide bridge, which leads to a mixed disulfide between both proteins and the regeneration of free Cys^{47} in Px III. Finally, Cys^{43} of Tpx attacks its vicinal Cys^{40} to release oxidized Tpx and the reduced Px III that is ready for the next round of catalysis. The catalytic mechanism of Px III shows some similarities to that of atypical 2-Cys-peroxiredoxins but there are also significant differences. For the atypical 2-Cys-peroxiredoxin from *Mycobacterium tuberculosis* it has been shown that the peroxidative Cys^{60} is attacked by both the oxidizing hydroperoxide substrate and the reducing thioredoxin. It has been suggested that the role of the third cysteine (Cys^{93}) is to prevent inactivation of the enzyme by over-oxidation of Cys^{60} under a restricted supply of reducing substrate [40]. As shown here, in Px III, Cys^{47} reacts with the hydroperoxide but Cys^{95} is attacked by Tpx.

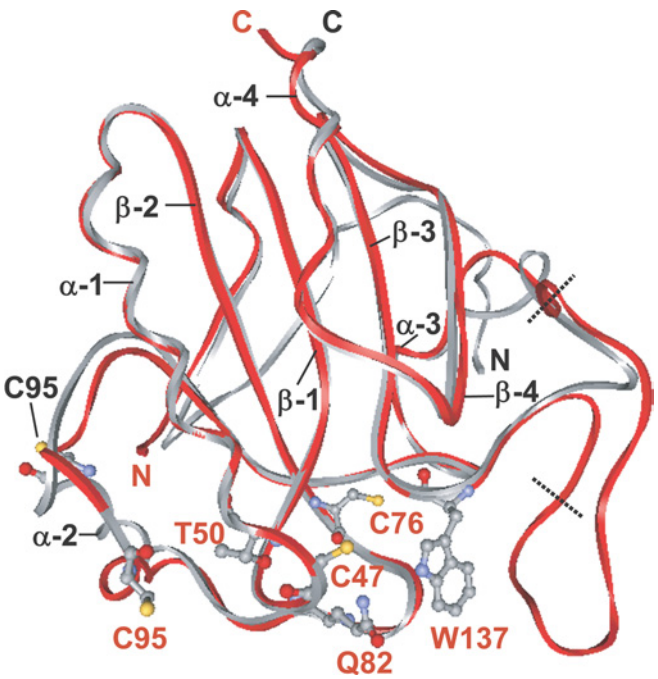

Figure 6 Three-dimensional model of Px III

The crystal structures of bovine erythrocyte GPX-1 (PDB 1GP1) and human GPX-4 (PDB 2GS3) served as templates to generate three-dimensional models of Px III. The ribbon representation of the C^{α}-superposition of the model based on the GPX-1 and GPX-4 structure is depicted in red and grey respectively. α-Helices and β-strands are numbered according to the structure of the bovine enzyme [24]. N and C denote the N- and C-termini of the models. Residues of Px III that were mutated in the present study (Table 1; Figure 1) are given as ball and stick models. The dotted lines mark the 18 residues of the bovine protein that were introduced in the *T. brucei* sequence to allow modelling of the C-terminal part of the parasite Px III. The Figure was produced using the program 3D-Mol (*Vector*-NTI Advance, Invitrogen).

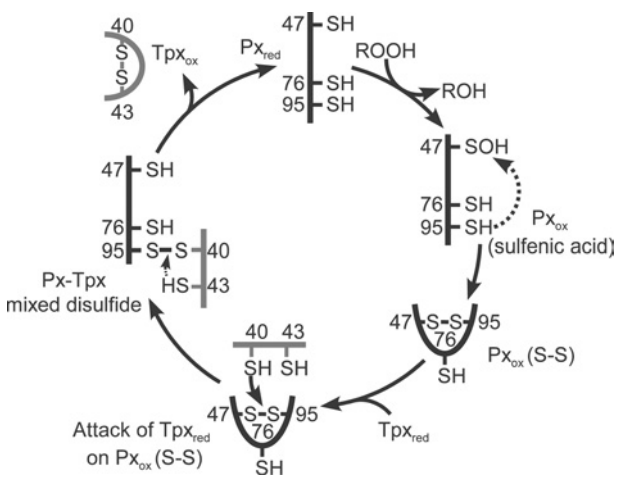

Figure 7 Proposed reaction mechanism of Px III

In the first half reaction, reduced Px III (Px_{red}) reacts with the hydroperoxide substrate and Cys^{47} becomes oxidized to a sulfenic acid [Px_{ox} (sulfenic acid)]. Attack of Cys^{95} leads to formation of an intramolecular disulfide between Cys^{47} and Cys^{95} [Px_{ox} (S-S)]. In the second half reaction, Cys^{40} of reduced Tpx (Tpx_{red}) attacks Cys^{95} of the disulfide bond resulting in an intermolecular disulfide between both proteins (Px–Tpx mixed disulfide). Cys^{43} of Tpx finally reacts with its vicinal Cys^{40} to release Px_{red} and oxidized Tpx (Tpx_{ox}). The different protein species, except for the sulfenic acid intermediate, have been experimentally demonstrated.

Outlook

In vitro, Px III catalyses the detoxification of different hydroperoxide substrates [7,8]. Its catalytic efficiency is comparable with that of the cytosolic 2-Cys-peroxiredoxin of the parasite but by orders of magnitude lower than those of catalase and GPXs that are missing in trypanosomes [3,7,8]. Both types of Tpx peroxidases are essential for *T. brucei* [8,11]. Obviously the highly abundant 2-Cys-peroxiredoxin cannot functionally substitute for the glutathione peroxidase-type enzyme(s) and vice versa. Since RNA interference does not distinguish between the three putative mRNAs a compartment-specific function of Px III is feasible. Another possibility is that the enzyme has functions distinct from or in addition to the detoxification of low-molecular-mass hydroperoxides. For the yeast glutathione peroxidase-type peroxidase-3, it has been shown that the enzyme acts not only as a hydroperoxide scavenger but also as a hydroperoxide sensor [14]. A sulfenic acid generated in the peroxidase reacts with a cysteine of Yap1 to a mixed disulfide followed by its conversion into an intramolecular disulfide of the activated regulator protein. Work is in progress to elucidate potential protein partners of the glutathione peroxidase-type Tpx peroxidases in *T. brucei*. Aim is to reveal if these essential enzymes act only as direct peroxidases or if they play a regulatory role in the redox metabolism of the parasites.

The plasmids for the expression of the cysteine mutants of *T. brucei* Tpx were kindly provided by Dr Leopold Flohé (MOLISA GmbH, Magdeburg, Germany). M.A.C. is a Research Fellow of the Medical Faculty of Heidelberg University. Our work is supported by the Deutsche Forschungsgemeinschaft (Sonderforschungsbereich 544 'Control of Tropical Infectious Diseases', project B3).

REFERENCES

1 Fairlamb, A. H. and Cerami, A. (1992) Metabolism and functions of trypanothione in the Kinetoplastida. Annu. Rev. Microbiol. **46**, 695–729
2 Krauth-Siegel, R. L., Bauer, H. and Schirmer, R. H. (2005) Dithiol proteins as guardians of the intracellular redox milieu in parasites: old and new drug targets in trypanosomes and malaria-causing plasmodia. Angew. Chem. Int. Ed. Engl. **44**, 690–715
3 Nogoceke, E., Gommel, D. U., Kiess, M., Kalisz, H. M. and Flohé, L. (1997) A unique cascade of oxidoreductases catalyses trypanothione-mediated peroxide metabolism in *Crithidia fasciculata*. Biol. Chem. **378**, 827–836
4 Tetaud, E., Giroud, C., Prescott, A. R., Parkin, D. W., Baltz, D., Biteau, N., Baltz, T. and Fairlamb, A. H. (2001) Molecular characterisation of mitochondrial and cytosolic trypanothione-dependent tryparedoxin peroxidases in *Trypanosoma brucei*. Mol. Biochem. Parasitol. **116**, 171–183
5 Flohé, L., Budde, H., Bruns, K., Castro, H., Clos, J., Hofmann, B., Kansal-Kalavar, S., Krumme, D., Menge, U., Plank-Schumacher, K. et al. (2002) Tryparedoxin peroxidase of *Leishmania donovani*: molecular cloning, heterologous expression, specificity, and catalytic mechanism. Arch. Biochem. Biophys. **397**, 324–335
6 Wilkinson, S. R., Meyer, D. J., Taylor, M. C., Bromley, E. V., Miles, M. A. and Kelly, J. M. (2002) The *Trypanosoma cruzi* enzyme TcGPXI is a glycosomal peroxidase and can be linked to trypanothione reduction by glutathione or tryparedoxin. J. Biol. Chem. **277**, 17062–17071
7 Hillebrand, H., Schmidt, A. and Krauth-Siegel, R. L. (2003) A second class of peroxidases linked to the trypanothione metabolism. J. Biol. Chem. **278**, 6809–6815
8 Schlecker, T., Schmidt, A., Dirdjaja, N., Voncken, F., Clayton, C. and Krauth-Siegel, R. L. (2005) Substrate specificity, localization, and essential role of the glutathione peroxidase-type tryparedoxin peroxidases in *Trypanosoma brucei*. J. Biol. Chem. **280**, 14385–14394
9 Gommel, D. U., Nogoceke, E., Morr, M., Kiess, M., Kalisz, H. M. and Flohé, L. (1997) Catalytic characteristics of tryparedoxin. Eur. J. Biochem. **248**, 913–918
10 Comini, M. A., Krauth-Siegel, R. L. and Flohé, L. (2007) Depletion of the thioredoxin homologue tryparedoxin impairs antioxidative defence in African trypanosomes. Biochem. J. **402**, 43–49
11 Wilkinson, S. R., Horn, D., Prathalingam, S. R. and Kelly, J. M. (2003) RNA interference identifies two hydroperoxide metabolizing enzymes that are essential to the bloodstream form of the African trypanosome. J. Biol. Chem. **278**, 31640–31646
12 Brigelius-Flohé, R. and Flohé, L. (2003) Is there a role of glutathione peroxidases in signaling and differentiation? Biofactors **17**, 93–102

13 Maiorino, M., Aumann, K. D., Brigelius-Flohé, R., Doria, D., van den Heuvel, J., McCarthy, J., Roveri, A., Ursini, F. and Flohé, L. (1995) Probing the presumed catalytic triad of selenium-containing peroxidases by mutational analysis of phospholipid hydroperoxide glutathione peroxidase (PHGPx). Biol. Chem. Hoppe Seyler **376**, 651–660
14 Delaunay, A., Pflieger, D., Barrault, M. B., Vinh, J. and Toledano, M. B. (2002) A thiol peroxidase is an H_2O_2 receptor and redox-transducer in gene activation. Cell **111**, 471–481
15 Jung, B. G., Lee, K. O., Lee, S. S., Chi, Y. H., Jang, H. H., Kang, S. S., Lee, K., Lim, D., Yoon, S. C., Yun, D. J. et al. (2002) A Chinese cabbage cDNA with high sequence identity to phospholipid hydroperoxide glutathione peroxidases encodes a novel isoform of thioredoxin-dependent peroxidase. J. Biol. Chem. **277**, 12572–12578
16 Tanaka, T., Izawa, S. and Inoue, Y. (2005) GPX2, encoding a phospholipid hydroperoxide glutathione peroxidase homologue, codes for an atypical 2-Cys peroxiredoxin in *Saccharomyces cerevisiae*. J. Biol. Chem. **280**, 42078–42087
17 Fomenko, D. E. and Gladyshev, V. N. (2003) Identity and functions of CxxC-derived motifs. Biochemistry **42**, 11214–11225
18 Lüdemann, H., Dormeyer, M., Sticherling, C., Stallmann, D., Follmann, H. and Krauth-Siegel, R. L. (1998) *Trypanosoma brucei* tryparedoxin, a thioredoxin-like protein in African trypanosomes. FEBS Lett. **431**, 381–385
19 Sullivan, F. X. and Walsh, C. T. (1991) Cloning, sequencing, overproduction and purification of trypanothione reductase from *Trypanosoma cruzi*. Mol. Biochem. Parasitol. **44**, 145–147
20 Reckenfelderbäumer, N. and Krauth-Siegel, R. L. (2002) Catalytic properties, thiol p*K* value, and redox potential of *Trypanosoma brucei* tryparedoxin. J. Biol. Chem. **277**, 17548–17555
21 Budde, H., Flohé, L., Hecht, H. J., Hofmann, B., Stehr, M., Wissing, J. and Lünsdorf, H. (2003) Kinetics and redox-sensitive oligomerisation reveal negative subunit cooperativity in tryparedoxin peroxidase of *Trypanosoma brucei brucei*. Biol. Chem. **384**, 619–633
22 Ellman, G. L. (1959) Tissue sulfhydryl groups. Arch. Biochem. Biophys. **82**, 70–77
23 Rist, W., Mayer, M. P., Andersen, J. S., Roepstorff, P. and Jorgensen, T. J. (2005) Rapid desalting of protein samples for on-line microflow electrospray ionization mass spectrometry. Anal. Biochem. **342**, 160–162
24 Epp, O., Ladenstein, R. and Wendel, A. (1983) The refined structure of the selenoenzyme glutathione peroxidase at 0.2-nm resolution. Eur. J. Biochem. **133**, 51–69
25 Altschul, S. F., Gish, W., Miller, W., Myers, E. W. and Lipman, D. J. (1990) Basic local alignment search tool. J. Mol. Biol. **215**, 403–410
26 Schwede, T., Kopp, J., Guex, N. and Peitsch, M. C. (2003) SWISS-MODEL: an automated protein homology-modeling server. Nucleic Acids Res. **31**, 3381–3385
27 Guex, N. and Peitsch, M. C. (1997) SWISS-MODEL and the Swiss-PdbViewer: an environment for comparative protein modeling. Electrophoresis **18**, 2714–2723
28 Maiorino, M., Ursini, F., Bosello, V., Toppo, S., Tosatto, S. C., Mauri, P., Becker, K., Roveri, A., Bulato, C., Benazzi, L. et al. (2007) The thioredoxin specificity of *Drosophila* GPx: a paradigm for a peroxiredoxin-like mechanism of many glutathione peroxidases. J. Mol. Biol. **365**, 1033–1046
29 Sztajer, H., Gamain, B., Aumann, K. D., Slomianny, C., Becker, K., Brigelius-Flohé, R. and Flohé, L. (2001) The putative glutathione peroxidase gene of *Plasmodium falciparum* codes for a thioredoxin peroxidase. J. Biol. Chem. **276**, 7397–7403
30 Tang, L., Gounaris, K., Griffiths, C. and Selkirk, M. E. (1995) Heterologous expression and enzymatic properties of a selenium-independent glutathione peroxidase from the parasitic nematode *Brugia pahangi*. J. Biol. Chem. **270**, 18313–18318
31 Alphey, M. S., Leonard, G. A., Gourley, D. G., Tetaud, E., Fairlamb, A. H. and Hunter, W. N. (1999) The high resolution crystal structure of recombinant *Crithidia fasciculata* tryparedoxin-I. J. Biol. Chem. **274**, 25613–25622
32 Budde, H., Flohé, L., Hofmann, B. and Nimtz, M. (2003) Verification of the interaction of a tryparedoxin peroxidase with tryparedoxin by ESI–MS/MS. Biol. Chem. **384**, 1305–1309
33 Laskowski, R. A., MacArthur, M. W., Moss, D. S. and Thornton, J. M. (1993) PROCHECK – a program to check the stereochemical quality of protein structures. J. Appl. Crystallogr. **26**, 283–291
34 Choi, J., Choi, S., Cha, M. K., Kim, I. H. and Shin, W. (2003) Crystal structure of *Escherichia coli* thiol peroxidase in the oxidized state: insights into intramolecular disulfide formation and substrate binding in atypical 2-Cys peroxiredoxins. J. Biol. Chem. **278**, 49478–49486
35 Rho, B. S., Hung, L. W., Holton, J. M., Vigil, D., Kim, S. I., Park, M. S., Terwilliger, T. C. and Pédelacq, J. D. (2006) Functional and structural characterization of a thiol peroxidase from *Mycobacterium tuberculosis*. J. Mol. Biol. **361**, 850–863
36 Declercq, J. P., Evrard, C., Clippe, A., Stricht, D. V., Bernard, A. and Knoops, B. (2001) Crystal structure of human peroxiredoxin 5, a novel type of mammalian peroxiredoxin at 1.5 Å resolution. J. Mol. Biol. **311**, 751–759
37 Mauri, P., Benazzi, L., Flohé, L., Maiorino, M., Pietta, P. G., Pilawa, S., Roveri, A. and Ursini, F. (2003) Versatility of selenium catalysis in PHGPx unraveled by LC/ESI–MS/MS. Biol. Chem. **384**, 575–588
38 Hofmann, B., Hecht, H. J. and Flohé, L. (2002) Peroxiredoxins. Biol. Chem. **383**, 347–364
39 Choi, H. J., Kang, S. W., Yang, C. H., Rhee, S. G. and Ryu, S. E. (1998) Crystal structure of a novel human peroxidase enzyme at 2.0 Å resolution. Nat. Struct. Biol. **5**, 400–406
40 Trujillo, M., Mauri, P. L., Benazzi, L., Comini, M., DePalma, A., Flohé, L., Radi, R., Stehr, M., Singh, M., Ursini, F. and Jaeger, T. (2006) The mycobacterial thioredoxin peroxidase can act as a one-cysteine peroxiredoxin. J. Biol. Chem. **281**, 20555–20566

Received 19 February 2007/13 April 2007; accepted 25 April 2007
Published as BJ Immediate Publication 25 April 2007, doi:10.1042/BJ20070259